Haber, D. A., Beverly, S. M., Kiely, M. L., & Schimke, R. T. (1981) *J. Biol. Chem. 256*, 9501–9510.
Hendrickson, S. L., Wu, J. R., & Johnson, L. F. (1980) *Proc. Natl. Acad. Sci. U.S.A. 77*, 5140–5144.
Johnson, L. F., Fuhram, C. L., & Weidman, L. M. (1978) *J. Cell. Physiol. 97*, 397–406.
Kaufman, R. J., & Sharp, P. A. (1983) *Mol. Cell. Biol. 3*, 1598–1608.
Kaufman, R. J., Brown, P. C., & Schimke, R. T. (1979) *Proc. Natl. Acad. Sci. U.S.A. 76*, 5669–5673.
Kellems, R. E., Alt, F. W., & Schimke, R. T. (1976) *J. Biol. Chem. 251*, 6987–6993.
Kellems, R. E., Morhenn, V. B., Pfendt, E. A., Alt, F. W., & Schimke, R. T. (1979) *J. Biol. Chem. 255*, 309–318.
Lachman, H. M., & Skoultchi, A. I. (1984) *Nature (London) 310*, 592–594.
Lewin, B. (1980) in *Gene Expression 2*, 2nd ed., Wiley, New York.
Leys, E. J., & Kellems, R. E. (1981) *Mol. Cell. Biol. 1*, 961–971.
Leys, E. J., Crouse, G. F., & Kellems, R. E. (1984) *J. Cell Biol. 99*, 180–187.
Loritz, F., Bernstein, A., & Miller, R. G. (1977) *J. Cell. Physiol. 90*, 423–438.
Marks, P. A., & Rifkind, R. A. (1978) *Annu. Rev. Biochem. 47*, 419–448.
Marks, P. A., Chen, Z.-X., Banks, J., & Rifkind, R. A. (1983) *Proc. Natl. Acad. Sci. U.S.A. 80*, 2281–2284.
Matews, C. K., Scrigmeour, K. G., & Huennekens, F. M. (1963) *Methods Enzymol. 6*, 364–368.
Melera, P. W., Lewis, J. A., Beidler, J. L., & Hession, C. (1980) *J. Biol. Chem. 255*, 7024–7028.
Nagi, J., Capetanaki, Y. G., & Lazarides, E. (1984) *J. Cell Biol. 99*, 306–314.
Neinhuis, A. W., Bunn, H. F., Turner, P. A., Gopal, T. V., Nash, W. G., O'Brien, S. J., & Sherr, C. J. (1985) *Cell (Cambridge Mass.) 42*, 421–428.
Nunberg, J. H., Kaufman, R. J., Chang, A. C. Y., Cohen, S. N., & Schimke, R. T. (1980) *Cell (Cambridge, Mass.) 19*, 355–364.
Schimke, R. T. (1981) *Harvey Lect. 76*, 1–25.
Schimke, R. T. (1984) *Cell (Cambridge, Mass.) 37*, 705–713.
Shen, D. W., Real, F. X., DeLeo, A. B., Old, L. J., Marks, P. A., & Rifkind, R. A. (1983) *Proc. Natl. Acad. Sci. U.S.A. 80*, 5919–5922.
Sherton, C. C., & Kabat, D. (1976) *Dev. Biol. 48*, 118–131.
Sirotnak, F. M., Moccio, D. M., Kelleher, L. E., & Goutas, L. J. (1981) *Cancer Res. 41*, 4447–4452.
White, B. A., & Bancroft, F. C. (1982) *J. Biol. Chem. 257*, 8669–8672.
Wu, J.-S. R., Weidemann, L. M., & Johnson, L. F. (1982) *Exp. Cell Res. 141*, 159–164.

Extended X-ray Absorption Fine Structure Studies of Zn_2Fe_2 Hybrid Hemoglobins: Absence of Heme Bond Length Changes in Half-Ligated Species†

K. Simolo,‡ Z. R. Korszun,§ G. Stucky,‡ K. Moffat,*,‖ and G. McLendon*,‡

Department of Chemistry, University of Rochester, Rochester, New York 14627, Section of Biochemistry, Molecular & Cell Biology, Cornell University, Ithaca, New York 14853, and Department of Chemistry, University of Wisconsin—Parkside, Kenosha, Wisconsin 53141

Appendix

G. Bunker

Institute for Structural and Functional Studies, 3401 Market Street, Philadelphia, Pennsylvania 19104

Received November 8, 1984; Revised Manuscript Received January 14, 1986

ABSTRACT: Metal hybrid hemoglobins, in which Zn(II) replaces Fe(II), have been structurally characterized by extended X-ray absorption structure (EAFS) studies. Since Zn and Fe have very different K absorption edge energies, the structures of the ligated (Fe) and unligated (Zn) sites could be examined independently within a single molecule that mimics an intermediate ligation state. The observed EXAFS spectra and associated structural parameters are compared among the ligand free $(\alpha Zn)_2(\beta Zn)_2$, half-ligated $(\alpha FeCO)_2(\beta Zn)_2$ and $(\alpha Zn)_2(\beta FeCO)_2$, and fully ligated $(\alpha FeCO)_2(\beta FeCO)_2$ systems.

Hemoglobin has long served as a paradigm for cooperative ligand binding in proteins (Antonini et al., 1971, Edelstein, 1975). However, the detailed mechanism of hemoglobin cooperativity remains controversial. A number of specific mechanisms have been proposed (Monod et al., 1965; Koshland et al., 1965; Gelin & Karplus, 1977; Warshel, 1977; Perutz, 1976). Perhaps the best known model is the "tension" or restraint model of Hoard and Perutz (Hoard, 1971; Perutz, 1976). In this model, the protein can adopt two quaternary structures corresponding to the MWC model (Monod et al., 1965). In the ligand-free (T) structure, this model suggests that the tension is localized in the $Fe-N_{Im}$ bond because the Fe atom is forced out of the plane of the heme while the protein restrains the axial imidazole ligand from its normal binding position. As ligands are successively added to the protein, the specific interactions that stabilize the T quaternary structure

† This research was supported through NIH Grants HL21461 (G.M.), GM29044 (K.M.), and GM32692 (Z.R.K.).
‡ University of Rochester.
§ University of Wisconsin—Parkside.
‖ Cornell University.

0006-2960/86/0425-3773$01.50/0

are lost, relieving the protein constraint and consequently increasing oxygen affinity. However, in an extended X-ray absorption fine structure (EXAFS) study (Eisenberger et al., 1976) comparing the low-affinity deoxyhemoglobin A to the high-affinity mutant deoxyhemoglobin Kempsey showed that the Fe–N_{pyr} and Fe–N_{1m} bond lengths were identical in these proteins to within experimental error. Thus, if stress is imposed by the globin on the heme or its axial ligands, it is not manifested in strain in the Fe–N bonds in the deoxy molecule.

In an alternative model, Gelin and Karplus (1977) have suggested that destabilization of the ligated T structure, as in partially ligated intermediates, is responsible for the low affinity of deoxyhemoglobin. That is, significant strain is to be sought not in the unligated, fully deoxygenated T structure but in the partially ligated T structure. Very recently, Brzozowski et al. (1984) have described a crystallographic study of an unusual, partially ligated hemoglobin in the T structure, $(\alpha FeO_2)_2(\beta Fe)_2$. This study suggests that the iron-proximal histidine bond in the oxygenated α-hemes is appreciably larger (2.4 Å) than the *normal value* (2.0 Å) and that both α-hemes are distinctly nonplanar. Indeed, the iron-proximal histidine bond length in one β-heme exceeds even the *normal value* (2.2 Å) for deoxyheme and is suggestive of appreciable strain.

At present it is not possible to convincingly argue that any of the proposed hypotheses is best at describing cooperativity in hemoglobin in terms of heme stereochemistry. In particular, it is highly desirable to know the heme stereochemistry of ligated and deoxyhemoglobin in both the R and T quaternary structures in order to determine the effect of heme stereochemistry on cooperativity. Additionally, differences in heme stereochemistry between the α and β chains of hemoglobin may also be important determinants of cooperativity. By substitution of various 3d transition metals such as Mn, Co, and Zn for the Fe atoms in hemoglobin, it is possible to affect the cooperativity of the hemoglobin tetramer. In addition, by substitution of different metals in the α vs. the β chains, it is possible to distinguish the effect that the chain differences may have upon cooperativity. When well-established techniques of metal substitution are applied (Scholler et al., 1978; Fiechtner et al., 1980a,b), it is possible to replace the normal Fe(II) by Zn(II) and prepare the hybrid hemoglobins $(\alpha Zn)_2(\beta FeCO)_2$ and $(\alpha FeCO)_2(\beta Zn)_2$. Zinc(II) porphyrins are 5-coordinate and are virtually isostructural with deoxy Fe(II) porphyrins (Hoard, 1976). Since the zinc(II) X-ray absorption edge is well separated from Fe, it is possible to monitor how the unligated Zn porphyrin is affected by a neighboring, ligated Fe porphyrin. Similarly, the structure of the ligated (Fe) heme can also be monitored in the presence of the unligated (Zn) subunit. The structural details of these systems are reported here and compared with the heme structures of the fully ligated $(\alpha FeCO)_2(\beta FeCO)_2$ and unligated $(\alpha Zn)_2(\beta Zn)_2$ systems.

Materials and Methods

The metal-substituted hemoglobins $(\alpha Zn)_2(\beta Zn)_2$, $(\alpha Cn)_2(\beta FeCO)_2$, and $(\beta FeCO)_2(\beta Zn)_2$ were prepared as previously described (Fiechtner et al., 1980a,b; Simolo et al., 1985). Care was taken to prevent exposure of the samples to visible light. Visible spectra of the preparations (diluted to 10 μM) were taken *before and after X-irradiation.* No evidence for radiation damage was observed. EXAFS spectra were obtained at the Cornell High Energy Synchrotron Source (CHESS) using experimental procedures previously described (Korszun et al., 1982). Samples were approximately 5 mM in heme. Adequate S/N was obtained in ca. six to eight scans.

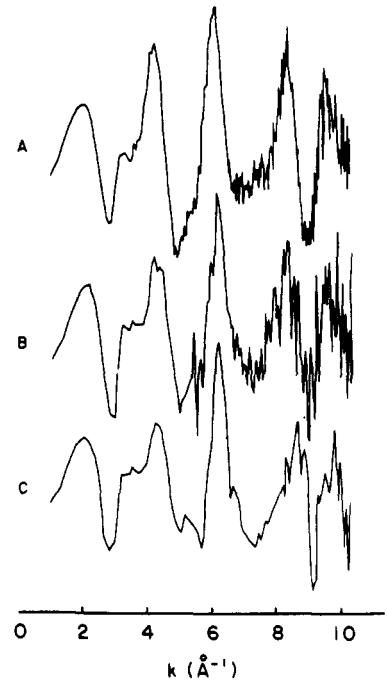

FIGURE 1: Fe EXAFS spectra. $k^2\chi(k)$ vs. k plots for $(\alpha FeCO)_2(\beta FeCO)_2$, $(\alpha Zn)_2(\beta FeCO)_2$, and $(\alpha FeCO)_2(\beta Zn)_2(\beta Zn)_2$ hemoglobin are shown as curves A–C. The abscissa has units of $Å^{-1}$, and the ordinate is in arbitrary normalized units. $k = 0.512(E - E_0)^{1/2}$.

Summed EXAFS spectra were normalized to their edge jumps, and E_0 was initially chosen as 7.110 keV for the Fe spectra and 9.665 keV for the Zn spectra. Each spectrum was subsequently converted to momentum (k) space with the Zn spectra multiplied by k^3 and the Fe spectra multiplied by k^2 in order to obtain amplitude functions which peak near the center of the k range utilized. This was followed by background removal where a splined polynomial was least squares fitted to the data using two sections. The background-corrected EXAFS spectra ranged from 1 to 10.5 $Å^{-1}$ where they were truncated because signal-to-noise ratios fall to between 2 and 3 (Stern & Heald, 1979). In addition to the protein spectra, data were collected on the pyridine adduct of zinc(II) tetrapyridylporphyrin (Py)Zn(TPyP). Data analysis followed procedures described by Lee et al. (1978). The background-corrected spectra were Fourier-transformed into distance (R) space, and a 1.5-Å wide Fourier transform window was used to isolate the first nearest-neighbor backscattering peak. The isolated peak was then back-transformed into k space, and the isolated first nearest-enighbor EXAFS spectra of the mixed-metal hemoglobin hybrids were compared to those of their corresponding pure metal hemoglobin molecules in a least-squares fit where ΔR, the difference in average distance of the first nearest neighbors, ΔA, their difference in amplitude, $\Delta\sigma^2$, the difference in the square of their Debye–Waller factors, and ΔE_0, their difference in threshold energy, were compared. In addition, the isolated back-transformed EXAFS spectra of the Zn-substituted hemoglobins were compared to the (Py)-Zn(TpyP) model compound.

Results

Figures 1 and 2 present the background-corrected Fe and Zn EXAFS spectra of the hemoglobin molecules used in this study. Figures 3 and 4 show the respective Fourier transformed spectra. Inspection of these figures illustrates the qualitative similarity of the Zn as well as the Fe backscattering environments independent of the metal substitution. Although the second and third backscattering shells are similar in Figure

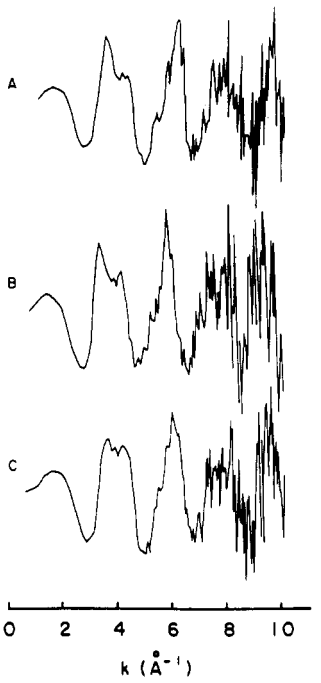

FIGURE 2: Zn EXAFS spectra. The curves of $k^2\chi(k)$ vs. k corresponding to $(\alpha Zn)_2\beta(Zn)_2$, $(\alpha Zn)_2(\beta FeCO)_2$, and $(\alpha FeCO)_2(\beta Zn)_2$ as indicated in Figure 1.

Table I: Least-Squares Analysis of Fe EXAFS Spectra[a]

	$(\alpha Zn)_2(\beta FeCO)_2$	$(\alpha FeCO)_2(\beta Zn)_2$
ΔR (Å)	−0.017 ± 0.015	−0.003 ± 0.015
ΔA	0.07 ± 0.1	−0.02 ± 0.10
$\Delta\sigma^2$	$-7.7 \times 10^{-5} \pm 8.0 \times 10^{-5}$	$3.8 \times 10^{-5} \pm 4.0 \times 10^{-5}$
ΔE_0 (eV)	−1.31	0.99

[a] The values presented are differences in the least-squares refinement parameters between the modified hemoglobin molecules and native $(\alpha FeCO)_2(\beta FeCO)_2$ hemoglobin. ΔR is the difference between the average first shell nearest-neighbors distances: αA is the difference in backscattering amplitude for the first shell peaks; $\Delta\sigma^2$ is the difference in their Debye–Waller Factors; ΔE_0 is the difference in their X-ray absorption thresholds. In all cases, a k range of 1–10 Å^{-1} was used.

3 and 4, systematic errors preclude quantitative analysis of second and third shells. The qualitative similarity within each class was verified quantitatively by using a nonlinear least-squares procedure. The first shells of the mixed metal hybrids were compared with the ligand-free $(\alpha Zn)_2(\beta Zn)_2$ and fully ligated $(\alpha FeCO)_2(\beta FeCO)_2$ species. Numeric results of this fit are presented in Tables I and II. The errors quoted in Tables I and II were calculated by systematically varying the appropriate parameter from its converged value until $\sum^2$, the sum of the squares of the residuals, reached twice its minimum value (Brown et al., 1980; W. E. Blumberg, unpublished observations). This procedure provides a profile of the least-squares minimum well with respect to the parameters varied. A measure of the precision of our measurements was obtained by separately analyzing several individual EXAFS scans of each particular species. Both methods of error analysis produced the consistent results listed in Tables I and II. A graphic illustration of representative fits is presented in Figures 5 and

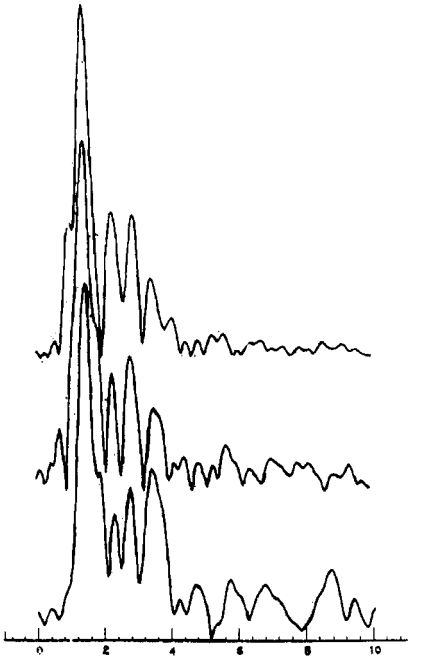

FIGURE 3: Fe Fourier transform magnitudes. The curves correspond to the respective species listed in Figure 1. The abscissa has units of angstroms with $R' = R + {}^1/_2 \langle d\alpha(k)/dk \rangle$ where $\alpha(k)$ is the appropriate phase shift function. The magnitudes are in normalized, arbitrary units and are directly comparable.

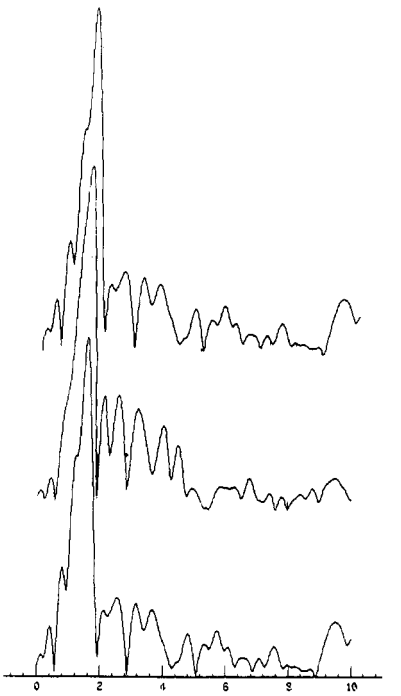

FIGURE 4: Zn Fourier transform magnitudes. The curves correspond to the respective species listed in Figure 1, and the units of the abscissa and ordinate are described in the caption of Figure 3.

Table II: Least-Squares Analysis of Zn EXAFS Spectra[a]

	$(\alpha FeCO)_2(\beta Zn)_2$	$(\alpha Zn)_2(\beta FeCO)_2$	(Py)Zn(TPyP)
ΔR (Å)	−0.010 ± 0.015	−0.020 ± 0.015	0.015 ± 0.015
ΔA	0.05 ± 0.10	−0.05 ± 0.10	0.25 ± 0.10
$\Delta\sigma^2$	$-1.7 \times 10^{-3} \pm 9.0 \times 10^{-4}$	$-1.1 \times 10^{-3} \pm 8.0 \times 10^{-4}$	$-1.5 \times 10^{-4} \pm 1.0 \times 10^{-4}$
ΔE (eV)	−0.10	−0.81	0.12

[a] The values presented are differences in least-squares refinement parameters of the partially substituted hemoglobin molecules and (Py)Zn(TPyP), using the fully substituted $(\alpha Zn)_2(\beta Zn)_2$ hemoglobin molecule as model. The entries are the same as those described in Table I. In all cases, a k range of 1–10 Å^{-1} was used.

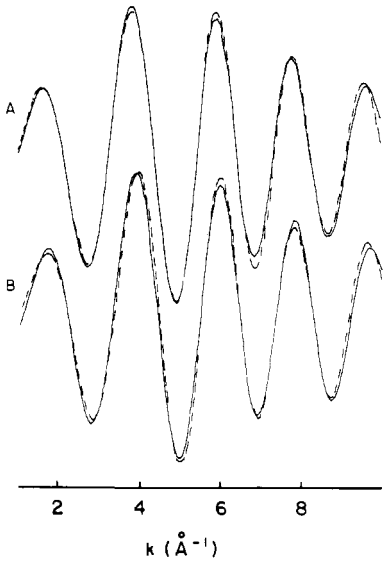

FIGURE 5: Comparison of Fe-filtered first shell EXAFS contributions. The solid curve is the spectrum of the $(\alpha FeCO)_2(\beta Zn)_2$ molecule (panel A) and the $(\alpha Zn)_2(\beta FeCO)_2$ molecule (panel B).

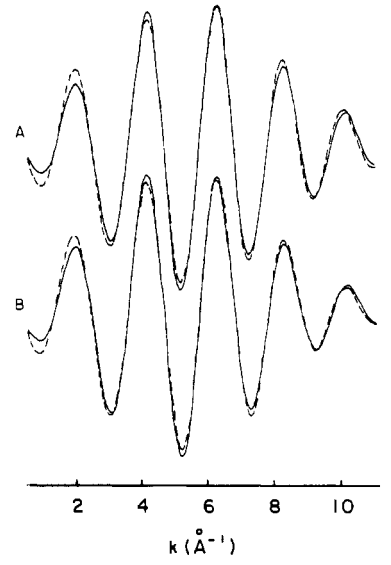

FIGURE 6: Comparison of Zn-filtered first shell EXAFS contributions. The solid curve is the spectrum of $(\alpha Zn)_2(\beta Zn)_2$ hemoglobin compared to the $(\alpha FeCO)_2(\beta Zn)_2$ molecule (panel A) and the $(\alpha Zn)_2(\beta FeCO)_2$ molecule (panel B).

6. Similar results were obtained in comparisons of $(\alpha Zn)_2(\beta FeCO)_2$ and $(\alpha FeCO)_2(\beta Zn)_2$ by using $(\alpha Zn)_2(\beta FeCO)_2$ as a model for $(\alpha FeCO)_2(\beta Zn)_2$. In general the fit of the filtered first nearest-neighbor backscattering contributions to the EXAFS spectrum was good in the range $1\ \text{Å}^{-1} \leq k \leq 10\ \text{Å}^{-1}$. The major uncertainty was observed in the amplitudes of the fitted functions. The results of this analysis suggest that the EXAFS for each metal data are consistent. That is, the pure metal spectra can be reproduced by the simple addition of the spectra from the mixed metal compounds to within an error of ±0.02 Å as measured in the Fourier transform of the synthetic spectra.

By use of the cumulant expansion method (Bunker, 1983), it is possible to derive a relationship between σ^2, the disorder parameter, and the maximum variation of the distances involved in the first nearest-neighbor backscattering peak for a simple yet physically important model. If a two distance model of identical backscattering atoms is used, then variation in σ^2 can be related to a difference in distances as derived in the Appendix. When this analysis is applied to the Zn hemoglobin EXAFS spectra with the assumptions that (1) all Zn–Npyr distances are equal, but not necessarily equal, to the Zn axial ligand distance and (2) the thermal disorder between $(\alpha Zn)_2(\beta Zn)_2$ and each of the mixed-metal hybrids cancels, then as derived in the Appendix

$$\bar{r} = [1/(1+\alpha)]r_{pyr} + [\alpha/(1+\alpha)]r_{Im} \quad (1)$$

$$(1+\alpha)\sigma = (\alpha)^{1/2}(r_{pyr} - r_{Im}) \quad (2)$$

As indicated in Table II, when the hemoglobin Zn EXAFS spectra are compared to the inorganic model compound (Py)Zn(TPyP), no significant differences in the refined parameters are observed. However, it is possible that significant differences in the stereochemistry of the heme metal group can nevertheless produce the same average distance (Eisenberger et al., 1978). Bunker has shown (Bunker, 1983) that $\bar{\gamma}$ and σ^2 completely characterize the complex first shell EXAFS spectrum. As will be discussed, this formulation of the problem provides bounds for the axial ligand distance consistent with the "Axial ligand corrections" used by Eisenberger et al. (1978). The Zn model compound has Zn–N_{pyr} bond lengths of 2.07 Å and an axial Zn–N_{py} bond length of 2.14 Å (Collins & Hoard, 1970). Given the crystallographic structure parameters, our data suggest that the average Zn–N_{pyr} bond lengths are 2.08 ± 0.02 Å and the Zn–N_{Im} bond length ranges between 2.15 and 2.24 Å as verified by substitution of the determined parameters and their associated errors into eq 1 and 2. This provides an independent measure of the accuracy of our measurements and suggests that, within the uncertainties quoted, the (Py)Zn(TPyP) compound is a good model for the Zn sites in the modified hemoglobins.

In the case of the Fe EXAFS spectra, it is more difficult to obtain a numeric estimate of possible differences in Fe–C and Fe–N bond lengths because the ligands are not identical. However, as indicated in Table I, differences in $\Delta\sigma^2$ are extremely small for the mixed-metal hybrids as compared to $(\alpha FeCO)_2(\beta FeCO)_2$, suggesting that differences in Fe stereochemistry must also be small.

Discussion

Extensive previous work has established many features of the ligation dynamics and solution structure of Fe, Zn hemoglobin hybrids. Functional studies of ligation kinetics (Simolo et al., 1985; Blough et al., 1980, 1981) show that both the CO off-rates and CO on-rates are significantly different on comparing the fully ligated $(\alpha FeCO)_2(\beta FeCO)_2$ ($k_{on} = 2 \times 10^6\ M^{-1}\ s^{-1}$; $k_{off} = 0.01\ s^{-1}$) to the half-ligated $Zn_2(FeCO)_2$ hemoglobins ($k_{on} = 1 \times 10^5\ M^{-1}\ s^{-1}$; $k_{off} = 0.11\ s^{-1}$). These kinetic studies establish that the half ligated hemoglobins have a low ligand affinity.

Within the limits of experimental uncertainty, the average Zn bond lengths are identical, for all of the zinc-substituted hemoglobin molecules used in this study. Comparison of the Zn protein data with the (Py)Zn(TPyP) model data suggests that the Zn stereochemistry in the proteins is similar to that of the model.

The Fe ligand stereochemistry is more difficult to determine in an EXAFS experiment because there are potentially three distances to fit to the data. It is, for example, possible that an increase in Fe–imidazole distance could be compensated by a decrease in Fe–pyrrole distance. However, such a trade off is quite unlikely, since in the transition from 6-coordination to 5-coordination, *all* Fe–ligand bond lengths increase (Rey and Ibers, 1976, Scheidt, 1977). Consequently, any change in stereochemistry of the hemes in the $(\alpha Zn)_2(\beta FeCO)_2$ or $(\alpha FeCO)_2(\beta Zn)_2$ hemoglobins would be expected to occur with

increases in the average Fe–ligand bond lengths. Since increases of greater than 0.02 Å in the average Fe–ligand bond lengths should be observable in our data, we conclude that the Fe environments in the hybrids are stereochemically similar to native carboxyhemoglobin.

Five-coordinate Zn porphyrins are virtually isostructural with five-coordinate (deoxy) Fe porphyrins (Scheidt, 1977), and Zn/Fe hybrids have been shown to bind CO with kinetics equivalent to low-affinity (deoxy)hemoglobin (Simolo et al., 1985). Thus, the $(\alpha FeCO)_2(\beta Zn)_2$ species is analogous to the unusual $(\alpha FeO_2)_2(\beta Fe)_2$ species studied crystallographically (Brzozowski et al., 1984). The structure of $(\alpha FeO_2)_2(\beta Fe)_2$ has been partially refined at 2.1-Å resolution. Brzozowski et al. report iron–proximal histidine bond lengths in the two crystallographically distinct oxygenated α-hemes of 2.10 and 2.39 Å. (Even larger values, 2.23 and 2.50 Å, are obtained by an alternative refinement strategy.) The latter bond is quite unusually long at 2.39 Å: corresponding values for oxyMb and oxyHb, obtained by using the same refinement strategy, are 2.07 (Mb), 1.94 (α), and 2.06 (β) Å, and 2.07 Å for the appropriate model heme.

The "restraint" model proposed by Perutz (1976) suggested that the protein restrains the heme (principally the heme imidazole bond), producing metal–ligand bond lengths (or angles) that differ in the low-affinity structure(s) from the bond lengths and angles in the fully relaxed high-affinity structure(s). Indeed, the heme stereochemistry of deoxyHb differs from that of the corresponding model heme; although bond lengths are closely comparable in the two structures, the proximal histidine is displaced appreciably off the heme normal in deoxyHb, with consequent alteration in certain bond angles. The present results show that there is no appreciable strain in the metal–ligand bond *distances* in any of the partially ligated hemoglobins. Iron–ligand bond lengths in the low-affinity half-ligated hybrid are closely similar (Table I) to those in the high-affinity, fully ligated $(\alpha FeCO)_2(\beta FeCO)_2$. Similarly, zinc–ligand bond lengths are similar in the half-ligated systems (Table II) to those in $(\alpha Zn)_2(\beta Zn)_2$, which is apparently isostructural by a range of solution criteria (NMR, CD, chemical reactivity) with deoxyHb (Simolo et al., 1985). In particular, there is no evidence for an unusually long iron–proximal histidine bond in either $(\alpha FeCO)_2(\beta Zn)_2$ or $(\alpha Zn)_2(\beta FeCO)_2$, although both species have a low affinity for CO, characteristic of the T state. If "proximal strain" is responsible for reducing the CO affinity of the $(FeCO)_2Zn_2$ hybrids, then this strain is not manifested in a bond length change. Angular strain *is* possible; ENDOR studies are in progress to test this possibility.

Finally, there are several possible explanations for the apparent discrepancy between these crystallographic and our EXAFS results on partially ligated species. First, $(\alpha FeCO)_2(\beta Zn)_2$ may not be a good stereochemical model for $(\alpha FeO_2)(\beta Fe)_2$. This seems unlikely since Zn porphyrins are excellent stereochemical mimics of (deoxy) Fe(II) porphyrins. Furthermore, $(\alpha Zn)_2(\beta Zn)_2$ is indistinguishable by high-resolution NMR in the frequencies of critical "salt links" from deoxyHb (Simolo et al., 1985) and crystallizes in the same space group as deoxyHb (G. McLendon, unpublished results). Second, the EXAFS analysis may be in error. EXAFS techniques inherently yield more precise values for metal–ligand bond lengths than do macromolecular crystallographic techniques. Furthermore, the likelihood for systematic errors in the EXAFS analysis, which would diminish its accuracy, is lessened in comparative studies of the type presented here. Third, crystallization may have favored a stereochemically unusual species, not normally well populated in solution. An influence of crystal lattice forces on heme stereochemistry might be inferred from the marked difference in iron–proximal histidine bond lengths in the two chemically identical but crystallographically distinct oxygenated α-hemes. Finally, further crystallographic refinement may indeed reveal a less unusual heme stereochemistry. Further work using both techniques is necessary to resolve the apparent discrepancy between the crystallographic and the EXAFS results.

Registry No. (Py)Zn(TpyP), 18581-77-6; Zn, 7440-66-6; N_2, 7727-37-9; heme, 14875-96-8; Fe, 7439-89-6.

REFERENCES

Antonini, E., & Brunori, M. (1971) *Hemoglobin and Myoglobin in their Reactions with Ligands*, North-Holland, London.

Blough, N. V., & Hoffman, B. M. (1982) *J. Am. Chem. Soc. 104*, 4247–4250.

Blough, N. V., Zemel, H., & Hoffman, B. M. (1980) *J. Am. Chem. Soc. 102*, 5683–5685.

Brown, J. M., Powers, L., Kincaid, B. M., Larrabee, J. A., & Spiro, T. G. (1980) *J. Am. Chem. Soc. 102*, 4210.

Brzozowski, A., Derewenda, Z., Dodson, E., Dodson, G., Grabowski, M., Liddington, R., Skarzynski, T., & Vallely, D. (1984) *Nature (London) 307*, 74–76.

Bunker, G. (1983) *Nucl. Instrum. Methods Phys. Res. 207*, 437–444.

Chance, B., Fischetti, R., & Powers, L. (1983) *Biochemistry 22*, 3820.

Collins, D. M., & Hoard, J. L. (1970) *J. Am. Chem. Soc. 92*, 3761.

Edelstein, S. J. (1975) *Annu. Rev. Biochem. 44*, 209–232.

Eisenberger, P. M., Shulman, R. G., Brown, G. S., & Ogawa, S. (1976) *Proc. Natl. Acad. Sci. U.S.A. 73*, 491.

Eisenberger, P., Shulman, R. G., Kincaid, B. M., Brown, G. S., & Ogawa, S. (1978) *Nature (London) 274*, 5666–5670.

Fiechtner, M. D., McLendon, G., & Bailey, M. W. (1980a) *Biochem. Biophys. Res. Commun. 92*, 277–284.

Fiechtner, M. D., McLendon, G., & Bailey, M. W. (1980b) *Biochem. Biophys. Res. Commun. 96*, 618–625.

Gelin, B. R., & Karplus, M. (1977) *Proc. Natl. Acad. Sci. U.S.A. 74*, 801–805.

Heidner, E. J., Ladner, R. C., & Perutz, M. R. (1976) *Mol. Biol. 104*, 707.

Hoard, J. L. (1971) *Science (Washington, D.C.) 174*, 1295–1302.

Hoard, J. L. (1976) in *Porphyrins and Metalloporphyrins* (Smith, K. M., Ed.) Elsevier, New York.

Korszun, Z. R., Moffat, K., Frank, K., & Cusanovich, M. A. (1982) *Biochemistry 21*, 2253–2258.

Koshland, D. E., Nemethy, G., & Filmer (1965) *Biochemistry 5*, 365–385.

Lee, P. A., Citrin, P. H., Eisenberger, P., & Kincaid, B. M. (1981) *Rev. Mod. Phys. 53*, 769.

Monod, J., Wyman, J., & Changeux, J. P. (1965) *J. Mol. Biol. 12*, 88–118.

Perg, S. M., & Ibers, J. A. (1976) *J. Am. Chem. Soc. 98*, 8032.

Perutz, M. F. (1976) *Br. Med. Bull. 32*, 195–208.

Perutz, M. F., Hasnain, S. S., Duke, P. J., Sessler, J. L., & Hahn, J. E. (1982) *Nature (London) 295*, 535–538.

Scheidt, W. R. (1977) *Acc. Chem. Res. 10*, 339–345.

Scheidt, W. R., & Reed, C. A. (1981) *Chem. Rev. 81*, 543–555.

Scholler, D. M., Wang, W. Y., & Hoffman, B. M. (1978) *Methods Enzymol. 52*, 487–493.

Simolo, K., Stucky, G., Chen, S., Bailey, M., Scholes, C., & McLendon, G. (1985) *J. Am. Chem. Soc. 107*, 2865–2872.
Stern, E. A., & Heald, S. M. (1979) *Rev. Sci. Instrum. 50*, 1579.
Warshel, A. (1977) *Proc. Natl. Acad. Sci. U.S.A. 74*, 1789–1793.

APPENDIX

The following discussion uses the terminology and notation of Bunker (1983). We wish to determine the position and width of a distribution composed of two subdistributions of identical atoms.

$$P(r)^{\text{total}} = P(r) + Q(r)$$

where

$$P(r) = \frac{(P)Np(P)(r)}{r^2} \exp(-2r/\lambda)$$

$$Q(r) = \frac{(Q)Np(Q)(r)}{r^2} \exp(-2r/\lambda)$$

$N^{(P)}p^{(P)}(r)\,dr$ is the probability of finding an atom in the interval $r + dr$ in distribution P, λ is the mean free path, and $\int p^{(P)}(r)\,dr = 1$; analogous expressions hold for distribution Q.

Let $P_n^{\text{total}} = \int P(r)^{\text{total}} r^n\,dr$, $p_n^{\text{total}} = P_n^{\text{total}}/P_0^{\text{total}}$, $P_n = \int P(r) r^n\,dr$, $P_n = P_n/P_0$, $Q_n = \int Q(r) r^n\,dr$, $q_n = Q_n/Q_0$; and $\alpha = Q_0/P_0$. The centroid $\bar{r}_0 P(r)^{\text{total}}$ is

$$\bar{r} = P_1^{\text{total}} = \frac{P_1 + Q_1}{P_0 + Q_0} = \left(\frac{1}{1+\alpha}\right) r^{(P)} + \left(\frac{\alpha}{1+\alpha}\right) r^{(Q)}$$

where $r^{(P)} = P_1$ and $r^{(Q)} = q_1$. Evidently the average position is just the weighted average of the positions of $P(r)$ and $Q(r)$. After some manipulation, the mean square width σ^2 can be expressed as

$$\sigma^2 = p^{\text{total}} - p_1^{\text{total}\,2} = \left(\frac{1}{1+\alpha}\right)^2 [\sigma^{(P)2} + \sigma^{(Q)2} + (r^{(P)} - r^{(Q)})^2 + \alpha^2 \sigma^{(Q)2}]$$

where $\sigma^{(P)2} = p_2 - p_1^2$ and $\sigma^{(Q)2} = q_2 - q_1^2$. These are the desired equations. Note the inequality $|r^{(P)} - r^{(Q)}| \leq [(1 + \alpha)/\alpha^{1/2}]\sigma$.

Conformational Analysis of Cholecystokinin CCK_{26-33} and Related Fragments by ^1H NMR Spectroscopy, Fluorescence-Transfer Measurements, and Calculations†

M. C. Fourniê-Zaluski,‡ J. Belleney,‡ B. Lux,§ C. Durieux,‡ D. Gêrard,§ G. Gacel,‡ B. Maigret,‖ and B. P. Roques*,‡

Département de Chimie Organique, U 266 INSERM et UA 498 CNRS, UER des Sciences Pharmaceutiques et Biologiques, 75006 Paris, France, Laboratoire de Physique UA 491 CNRS, UER des Sciences Pharmaceutiques, 67000 Strasbourg, France, and Laboratoire des Molécules Informatiques, Institut Le Bel, Université de Strasbourg I, 67008 Strasbourg, France

Received October 31, 1985; Revised Manuscript Received February 19, 1986

ABSTRACT: The conformational behavior of CCK_7, Tyr-Met-Gly-Trp-Met-Asp-Phe-NH_2, and CCK_8, Asp-Tyr-Met-Gly-Trp-Met-Asp-Phe-NH_2, in their sulfated and unsulfated forms, was studied both by ^1H NMR spectroscopy in dimethyl-d_6 sulfoxide and water and by fluorescence-transfer measurements at pH 7. In neutral conditions, both experimental methods show that these peptides exist preferentially in folded forms with β and γ turns around the sequence Gly-Trp-Met-Asp and Met-Asp-Phe-NH_2, respectively. The presence of stable folded conformations is supported by through-space effects during the titration of the ionizable groups and by the weak temperature dependency of some amide protons not only in dimethyl sulfoxide but also in water. The folding of the C-terminal part, already shown in CCK_5, seems to be a common conformational characteristic in CCK peptides. The N-terminal part of CCK_8 presents an equilibrium between β and γ turns, whereas this part of the peptide is more flexible in CCK_7. The low quantum yield of Tyr and the large mean distance (R = 15 Å) between Tyr and Trp, determined by fluorescence-transfer measurements, support the occurrence of folded conformations pushing the aromatic rings far from each other. Interestingly, the introduction of the sulfate group enhances the folding tendency even in aqueous medium. The larger amide temperature dependency and the decrease in the R distance at acidic pH suggest that an intramolecular ionic interaction involving the N-terminal amino group and the β-carboxyl groups of Asp^{32} stabilize the folded forms. Metropolis calculations performed on CCK_8 support the existence of stable folded conformations closely related to those deduced from experimental data. The conformationally constrained C-terminal part of CCK_8 and related peptides seems to play a crucial role in the efficient recognition of the brain receptors, whereas the observed external orientation of the sulfated tyrosine ring is probably required to induce the transduction process.

Cholecystokinin CCK (Ivy & Oldberg, 1928), originally described as a gut hormone (Mutt & Jorpes, 1971) and subsequently discovered in the brain (Vanderhaeghen et al., 1975; Rehfeld, 1978), is one of the most abundant peptides in the central nervous system (CNS), where it has recently been implicated as a putative neurotransmitter (Pinget et al., 1979; Dodd & Kelly, 1981). CCK exists in various molecular forms differing among species (Zhou et al., 1985), but the C-terminal octapeptide CCK_8 [Asp-Tyr(SO_3H)-Met-Gly-Trp-Met-Asp-Phe-NH_2], which retains all the activity of the entire hormone in the gastrointestinal tract (Ondetti et al., 1970), is the predominant form in the brain (Dockray, 1976). The struc-

† This research is supported by grants from Université René Descartes, Centre National de la Recherche Scientifique, and Institut National de la Santé et de la Recherche Médicale.
‡ UER des Sciences Pharmaceutiques et Biologiques.
§ UER des Sciences Pharmaceutiques.
‖ Université de Strasbourg I.

0006-2960/86/0425-3778$01.50/0